

PERSPECTIVES

Nano-to-Microscale Mechanical Switches and Fuses Mediate Adhesive Contacts between Leukocytes and the Endothelium

Volkmar Heinrich,^{*,†,#} Andrew Leung,[‡] and Evan Evans^{†,‡,§}

Department of Biomedical Engineering, Boston University, 44 Cummington Street, Boston, Massachusetts 02215, and Department of Pathology and Department of Physics and Astronomy, University of British Columbia, 2211 Wesbrook Mall, Vancouver, British Columbia V6T 2B5, Canada

Received May 9, 2005

INTRODUCTION

As a vital part of the inflammatory response, the leukocyte adhesion cascade involves the capture of white blood cells at the vascular endothelium, a progressively slowing, “rolling” motion of cells along the vessel walls, firm cell adhesion at target sites, and eventually, the transmigration of activated cells into the inflamed tissue^{1–4} (for an instructive overview see also <http://bme.virginia.edu/ley/>). Studies aiming to reveal the biophysical mechanisms underlying these processes face the difficult challenge of covering a large range of relevant scales: nanoscale interactions between adhesive molecules, local deformations of subcellular structures under point loads, and whole-cell activation and motion. Yet multiscale approaches also offer particularly rewarding insights, for example, by providing an understanding of single-molecule interactions within their natural, larger-scale biological context and, conversely, by tracing macroscopically observed cellular phenomena directly to their molecular origins.

The present work focuses on nano-to-microscale regulatory aspects that mediate the initial stages of the adhesion cascade. Early events, such as the capture of leukocytes and their initial rolling exploration at the endothelium, occur usually too fast to be regulated biologically, i.e., through the expression of proteins. We thus expected that most mechanisms governing initial leukocyte adhesion under a broad range of blood-flow conditions had to be “preprogrammed” into molecular-to-subcellular structures and that they had to be primarily mechanical. Accordingly, our experimental approach was to study in vitro the nano-to-micromechanical response of individual leukocytes that were loaded at a point with a rapidly increasing force.

The adhesion bond between P-selectin (expressed in vivo on the endothelium and on activated platelets), and its ligand PSGL-1 (resident in the leukocyte membrane) is a key player in the initial adhesion stages.^{4,5} We exploited this bond to form point attachments between polymorphonuclear leukocytes (PMNs) and functionalized microspheres that had been coated with P-selectin. To distinguish the dynamic properties of an individual P-selectin:PSGL-1 bond from mechanisms

governed by other cellular structures, we also tested this bond on its own using isolated PSGL-1 that had been immobilized on a second batch of microspheres.

Both types of interaction, i.e., P-selectin:PSGL-1 as well as P-selectin:PMN, were characterized by *dynamic force spectroscopy*^{6,7} over exceptionally wide ranges of force-loading rates. Complementary test surfaces were first brought into soft, feedback-controlled contact to allow for the formation of bonds between immobilized, reactive molecules. Then, while moving the surfaces apart at preset velocities, we recorded the force experienced by attachments between them. Piconewton forces were reported by the *biomembrane force probe*,^{8,9} a prototypical biophysical tool that is uniquely suited to study the dynamics of biologically relevant, ultraweak interactions.

This approach enabled us to inspect in detail two possible candidates for principal regulatory mechanisms in early leukocyte adhesion. One is a serial molecular attachment consisting of (i) the extracellular P-selectin:PSGL-1 bond and (ii) a putative, weak biochemical link that anchors the intracellular tail domain of the transmembrane PSGL-1 to the cortical cytostructure.¹⁰ The other is a hierarchy of rheological cell responses to point loads: from slow viscoelastic deformation of the whole cell, and a soft-elastic displacement of the cell cortex, to the extrusion of thin membrane tubes (“tethers”) that can easily grow—at quasi-constant pulling forces—to several micrometers in length. The formation of tethers from fluid membranes under point loads is a ubiquitous phenomenon, as evidenced by a large body of work on lipid vesicles^{11–14} and on various types of biological cells.^{15–18} A number of pioneering studies also investigated the mechanical properties of PMN tethers^{19–21} and their importance in leukocyte rolling.^{22,23}

Perhaps even more interesting than these regulatory mechanisms by themselves is the intriguing interplay between them. For example, the lifetime of weak attachments under stress depends critically on the history of force application. In the present case where the leukocyte itself links adhesive molecules to rigid surfaces, any subcellular soft structures will act to dampen the sudden impact of force and thus modulate the force history experienced by the actual adhesion bonds. Therefore, the lifetime, or strength, of adhesive attachments is directly affected by the rheology of cell deformation under point loads. On the other hand, the extrusion of tethers from PMNs appears to commence only

* Corresponding author e-mail: vheinrich@ucdavis.edu.

† Boston University.

Current address: Department of Biomedical Engineering, University of California, Davis, 451 East Health Sciences Drive, Davis, CA 95616.

‡ Department of Pathology, University of British Columbia.

§ Department of Physics and Astronomy, University of British Columbia.

after the cytoskeletal anchor of PSGL-1 has been released. This demonstrates how the failure of a nanoscale attachment may trigger the crossover between distinct regimes of the rheological response of the leukocyte, e.g., from soft-elastic displacement of the cell cortex to tether formation.

The present paper summarizes our recent results on a number of such mechanical, regulatory aspects of PMN adhesion that contribute to the stabilization of leukocyte rolling velocities within a narrow range despite wide variations in shear stresses.^{24–26} Technical and methodological details of our approach have been published before.^{24–27} Therefore, we will include here only the basic principles of experimental operation inasmuch as they are required to understand the interpretation of our results.

BACKGROUND

Dynamic Force Spectroscopy – A Generic Approach to Characterize Weak Interactions. Single-molecule force measurements have been performed with a variety of sensitive force-probe instruments. The required piconewton force resolution can be achieved, to varying degree, by the atomic force microscope (AFM), optical tweezers, the biomembrane force probe (BFP), magnetic pullers (often also called “magnetic tweezers”), and other force microscopes that have used specialized force transducers such as glass fibers or flow in a micropipet. The two most common protocols of force application using these instruments are force clamp and force ramp. Force clamps step up the applied force and then hold it constant at the desired value while recording distance changes that signify molecular events such as bond rupture or intramolecular transitions. In addition to changes in length, the quantity most interesting to assess molecular kinetics is simply the time that goes by until a transition occurs. On the other hand, force ramps increase the applied force gradually, preferably in a linear fashion. Since the applied force-loading rate is known, time and force are interchangeable (until a molecular transition occurs). It has become customary to record the transition force in this mode.

Since molecular-scale transitions are strongly mediated by the random impulses imparted by the thermal environment, lifetimes and transition forces are stochastic quantities. A large number of events need to be recorded to establish the most likely lifetime (at a given holding force) or transition force (at a given force-loading rate). Perhaps one of the most important fundamental insights gained from the interpretation of single-molecule force measurements is that the most likely transition force depends on the applied loading rate,⁶ just as the lifetime depends on the holding force. Therefore, the strength of a molecular interaction cannot be characterized by a single value of force. Any statement about the (most likely) rupture force of a weak molecular bond has to indicate, at the very least, the rate of force loading under which the force was measured. A more complete characterization of the molecular interaction must be based on measurements performed at a spectrum of loading rates (or holding forces). Dynamic force spectroscopy^{6,7} is a generic approach for the quantification of biomolecular interactions on the basis of such experimental spectra. It is independent of the particular force-probe instrument and has, indeed, been successfully used in the interpretation of data obtained with the BFP, AFM, optical tweezers, flow chambers, and other dynamic force techniques.

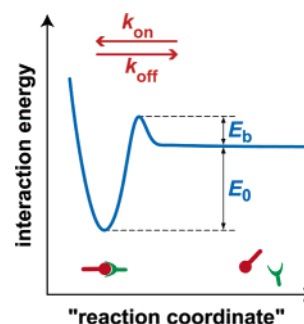


Figure 1. Schematic energy landscape governing the interaction of two biomolecules (pin and wedge symbols at the bottom).

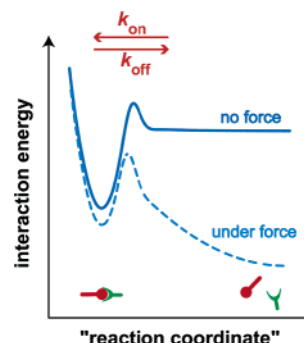


Figure 2. Schematic energy landscape governing the interaction of two biomolecules (solid line, cf. Figure 1) and the impact of a mechanical potential contributed by pulling with a force probe (dashed line).

We start from the conceptual view of an *energy landscape* that governs the interaction between biomolecules (including intramolecular configurational transitions), as has been common in chemical kinetics since Arrhenius and Eyring. The simplest possible energy landscape for the formation/release of a bond between two molecules is depicted schematically in Figure 1. It maps out the interaction energy along the optimum pathway of dissociation (the “reaction coordinate”). This path leads from a deep minimum—the bound state—over a single, sharp energy barrier to the free, unbound state. The rates of the unbinding (“forward”) and rebinding (“reverse”) transitions are given by (for notation see Figure 1)

$$k_{\text{off}} = A_{\text{off}} \exp\left(-\frac{E_0 + E_b}{k_B T}\right), \quad k_{\text{on}} = A_{\text{on}} \exp\left(-\frac{E_b}{k_B T}\right) \quad (1)$$

In solution, Eyring’s prescription for the empirical attempt frequencies (prefactors to the exponentials) has to be augmented by the Brownian damping due to the liquid environment. Kramers’ theory²⁸ has provided us with a physical basis for the interpretation of these prefactors in terms of the local diffusivity and of the shape of the energy landscape local to the minimum and the barrier.

Here, we are interested in the role of force, which primarily affects the exponentials. The main effect of adding the mechanical potential of a force probe to the interaction energy is a tilt in the energy landscape, pulling down the barrier as shown in Figure 2. (Small shifts in the positions of the minimum and the barrier can be neglected when dealing with deep, narrow minima and sharp barriers. We denote the fixed position of the barrier, or of the “transition state”, relative to the bound state by x_{ts} .) In the simplest case

of applying a force f that is roughly constant along the reaction coordinate, the reduction in barrier height, $-fx_{ts}$, is the dominating contribution to the change in the off-rate (eq 1):

$$k_{\text{off}}(f) = A_{\text{off}} \exp\left(-\frac{E_0 + E_b - fx_{ts}}{k_B T}\right) \quad (2)$$

Denoting the spontaneous off-rate $k_{\text{off},0} \equiv k_{\text{off}}(0)$, this is rewritten as

$$k_{\text{off}}(f) = k_{\text{off},0} \exp\left(\frac{fx_{ts}}{k_B T}\right) = k_{\text{off},0} \exp(f/f_\beta) \quad (3)$$

where the second equality introduces the characteristic force scale for rate exponentiation defined as $f_\beta \equiv k_B T/x_{ts}$. First proposed by Bell,²⁹ eq 3 clearly illustrates how force exponentially increases the rate of dissociation.

How can we make the connection between these general considerations and experimental force-ramp measurements that give us a distribution of transition forces? Reinterpreting traditional kinetic rate equations as master equations describing a Markov process, we may write for the present simple case

$$\frac{dS_0}{dt} = -k_{\text{off}}S_0 + k_{\text{on}}(1 - S_0) \quad (4)$$

S_0 is the normalized likelihood for occupancy of the bound state. Most force-probe experiments ramp the force too quickly, or use a clamping force too high, to allow rebinding. These experiments are thus performed *far from equilibrium*, causing the second term in eq 4 to vanish.

The solution of the remainder of eq 4 is nontrivial because k_{off} depends on force (cf. eq 3), which in turn depends on time. Considering linear ramps in force and denoting the loading rate $r_f \equiv f/t$, we find

$$\frac{dS_0}{df} = -\frac{k_{\text{off},0}S_0}{r_f} \exp(f/f_\beta) \quad (5)$$

The location of the peak in a measured distribution of transition forces can easily be calculated from eq 5 if one recognizes that the measured transition will occur most frequently at the force where the survival likelihood decreases most rapidly with force. Setting the derivative of eq 5 with respect to force to zero, and reinserting the original equation into the resulting right-hand side, we obtain for the most frequent transition force

$$f^* = f_\beta \ln\left(\frac{r_f/f_\beta}{k_{\text{off},0}}\right) \quad (6)$$

This hallmark result of DFS appeared first in 1997.⁶ It predicts a logarithmic dependence of the most frequent transition force f^* on the loading rate r_f for the simple case shown in Figure 2. It also clearly illustrates that *two* parameters are needed to characterize even the simplest biomolecular interaction: the generalized interaction strength given by the force scale f_β and the apparent unstressed off-rate (or inverse lifetime) $k_{\text{off},0}$.

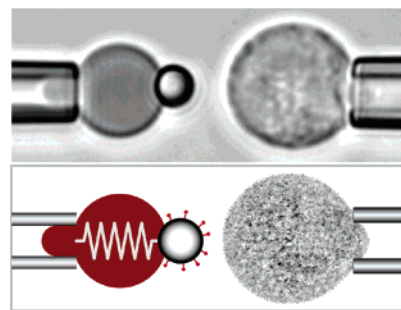


Figure 3. Video-micrograph (top)²⁵ and sketch (bottom) depicting a biomembrane force probe (BFP, on the left) and a test neutrophil held in a facing micropipet (on the right). The stationary BFP consists of a preswollen, pipet-aspirated red blood cell and a functionalized probe tip that is chemically glued to the red cell. A spring overlay in the sketch symbolizes Hookean behavior upon horizontal deflection. The probe tip is a glass microsphere that was coated with reactive molecules (denoted by pin-shaped symbols in the sketch). The neutrophil pipet (on the right) is mounted to a closed-loop piezo translator. The diameter of the spherical part of the red cell on the left is $\sim 6 \mu\text{m}$.

If a sufficiently large number of transition forces have been collected at each loading rate, the comparison of the measured histograms of forces with theoretical predictions can significantly increase the confidence in data interpretation. The probability density $\rho(f)$ for the transition to occur at the force f is simply the negative rate of change of the survival likelihood of the ground state, $\rho(f) = -dS_0/df$. The now-required solution of eq 5 is straightforward and leads to the *Evans distribution*⁷ of transition forces that can be written as

$$\rho(f) = C_s s \exp(-s) \quad \text{where} \quad s \equiv \exp\left(\frac{f - f^*}{f_\beta}\right) \quad (7)$$

with f^* given by eq 6. (The scaling prefactor $C_s \equiv \exp(f_\beta k_{\text{off},0}/r_f)/f_\beta$ has units of 1/force.) Whenever possible, this *universal* distribution should be matched to experimental transition-force histograms as a self-consistency test for the results.

The above treatment outlines the general approach to the quantitative interpretation of molecular force-probe experiments. For simplicity, we have considered only the simplest case where a single, sharp energy barrier impedes the unbinding of a weak molecular bond. A surprising amount of experimental data was found to be in excellent agreement with the predicted logarithmic dependence of the transition force on loading rate, eq 6. On the other hand, for molecular interactions with possible direct involvement in the regulation of biological processes one might expect a more complex behavior.

Biomembrane Force Probe – A Unique Instrument to Study the Dynamics of Ultraweak Interactions. Figure 3 illustrates the *biomembrane force probe* (BFP)⁸ as used in the present P-selectin:PMN tests. Originally designed and applied to measure the strength of single molecular bonds over an exceptional dynamic range (5–6 orders of magnitude in force-loading rate, with a damping factor as small as $\sim 0.0005 \text{ pNs/nm}$),⁷ the figure demonstrates how the BFP is also easily adopted for experiments probing the softness of linkers on various scales, including macromolecules, sub-cellular structures, or even whole cells.

On the left side of both parts of Figure 3, a stationary glass micropipet holds a partially aspirated, preswollen red blood cell to which a small glass bead—the probe tip—was glued chemically. The pressurized red cell is basically an empty membrane bag that behaves like an ideal Hookean spring when deformed along the axis of the rotationally symmetric assembly. A major advantage of the BFP over other piconewton force transducers is that it provides the experimentalist with a handle on its spring constant k_t . Not only is k_t known fairly accurately from membrane mechanics, it can even be adjusted over a considerable range (~ 0.1 – 5 pN/nm) by changing the suction pressure in the pipet that holds the red blood cell. Given by⁸

$$k_t \cong 2\pi \frac{\sigma}{\ln[4R_0^2/(R_p R_c)]} \quad (8)$$

the BFP spring constant depends on the membrane tension σ set by the aspiration pressure Δp through

$$\sigma = \frac{1}{2} \frac{R_0 R_p}{R_0 - R_p} \Delta p \quad (9)$$

and on three geometric parameters: the radius R_0 of the spherical portion of the aspirated cell (measured in the absence of an axial force), the radius R_p of the micropipet, and the radius R_c of the contact disk between red cell and probe-tip bead. A recent experimental study assessing the accuracy of eq 8 gave a sound confirmation of the validity of this equation.³⁰

Multiplying k_t by the deflection of the force transducer (red blood cell) gives force. The transducer deflection is determined from the displacement of the dark diffraction band at the rear of the probe tip. Optical microscopy (Carl Zeiss, Inc., Thornwood, NY) combined with fast video imaging (SensiCam, Cooke Corp., Auburn Hills, MI) allows us to track this diffraction pattern with a resolution of 5–10 nm at frame rates up to ~ 1500 frames per second (fps). The 50-fold increase in temporal resolution over the conventional video framing speed (30 fps) is critical for detection of events over a range of 5–6 orders of magnitude in force-loading rate. Monitoring the force in real time at ~ 0.6 -ms intervals has also enabled us to implement a fast feedback algorithm to control, for example, the impingement force upon touch of a test object to the transducer. Dedicated software allows us to set the approach speed, the feedback-controlled (negative) impingement force, duration of touch, and rate of force loading as needed in each experiment. At high pulling speeds the force reported by the BFP needs to be corrected for viscous damping. The damping coefficient of the (parallel) viscous component of the BFP transducer is easily determined from its exponentially decaying recoil after detachment from any test surface.^{7,27}

The probe tip is decorated with the receptor (here: P-selectin) for an adhesive molecule (here: PSGL-1) that is immobilized on a test surface. Using a second micropipet to hold and translate the test surface gives our setup great versatility. For example, the test surface can be the chemically modified surface of another glass bead, as in our P-selectin:PSGL-1 tests. Alternatively, as in the case shown in Figure 3, the membrane of an intact neutrophil can be used as the test surface, thus allowing us to study membrane-

based adhesion molecules in their natural environment. Translating this test surface into contact with the force probe and subsequently retracting it at the desired rate of force-loading allows us to determine the dynamic adhesion strength and, if needed, the softness of linkers. Translation with nanometer positioning accuracy is achieved by a closed-loop piezo actuator (Polytec PI, Inc., Auburn, MA).

A typical measurement runs for up to 500 test cycles, after which a new BFP (fresh red cell, probe bead, and test surface) is assembled before proceeding with the experiment. When probing dynamic bond strength, up to ~ 500 bond-failure forces are usually collected at each loading rate, ideally with an attachment frequency of $\sim 10\%$ of the total number of touches. This low bond frequency provides high confidence that the recorded attachments are mostly single bonds. (For example, assuming Poisson-distributed attachment events, the confidence for bonds to be single is 95% at an attachment frequency of 10%.⁷)

RESULTS

Figure 4 presents an overview of two different BFP experiments that we performed to test the P-selectin:PSGL-1 bond (Figure 4A) and the P-selectin:PMN interaction (Figure 4B). Force-time curves recorded during typical test cycles are shown at the bottom. Negative forces mark the feedback-controlled compression of the BFP spring as observed after the test surface had been translated into contact with the probe bead. Subsequently, the test surface was retracted at a preset “nominal” force-loading rate $r_f^0 \equiv k_t v_{\text{pull}}$ defined as the product of the BFP spring constant k_t and the piezo pulling speed v_{pull} . This retraction created an increasing force load on any adhesive attachments that had formed during the contact between the two reactive surfaces. The true loading rate experienced by all serial linkages during this stage is the local slope $r_f \equiv df/dt$ of the measured force-time curve. Final detachment of the BFP from the test surface was observed as the recoil of the BFP spring to zero force.

For bead-vs-bead tests such as in Figure 4A, the slope r_f of the linear force rise is roughly the same as the nominal loading rate r_f^0 . The maximum force immediately before detachment was recorded as the rupture force of an individual bond, tested at the given loading rate. Collecting a large number of P-selectin-PSGL-1 rupture forces over a wide range of loading rates and plotting the most frequent rupture forces as a function of the logarithm of the loading rate provided us with the dynamic force spectrum of this adhesion bond (see the next subsection).

The example curves in Figure 4B show intriguing force histories recorded in P-selectin:PMN tests at various nominal force-loading rates r_f^0 . Dotted lines indicate the behavior that one would expect for a rigid linkage where $r_f = r_f^0$. The measured forces rise considerably slower, which reflects linker softness—in this case, the softness of the PMN. At all loading rates, the typical force-time behavior of sufficiently long-lived attachments revealed two distinct regimes of PMN softness. The first was an initial elastic deformation of the cell cortex by ~ 200 – 500 nm, evident in the linear force rise up to the crossover force labeled f_ϕ . In the second regime beyond f_ϕ , the rheological response was a continually growing cell extension (up to several micrometers) at quasi-constant force, resembling plastic flow. At this stage,

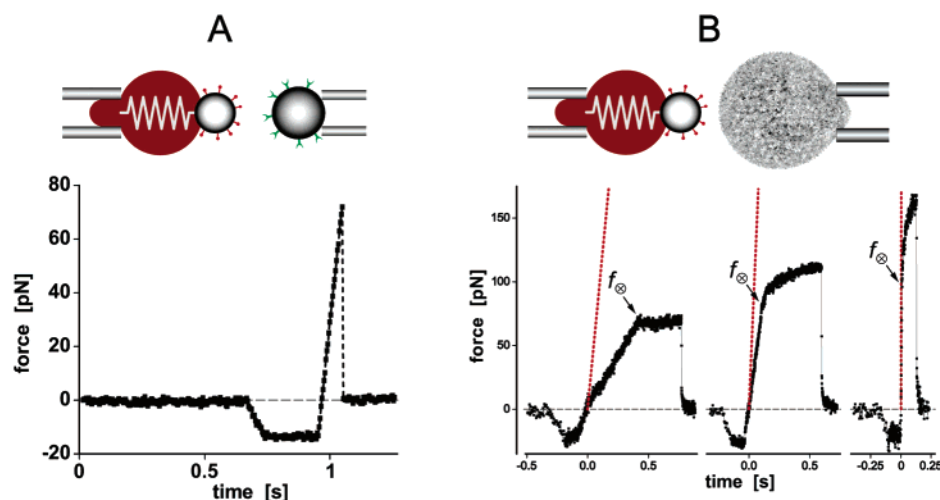


Figure 4. Sketches of BFP experiments (top) and force-time curves recorded during test cycles (bottom) for the P-selectin:PSGL-1 bond (A) and for the interaction between P-selectin and intact neutrophils (B).²⁶ In both cases, P-selectin (denoted by pin-shaped symbols) was immobilized on the probe-tip bead. The test surface in A is another glass bead coated with isolated PSGL-1 (wedge-shaped symbols). In B, the membrane of a pipet-held PMN represents the test surface. The difference between the force-time curve in A and the three example curves (taken at different force-loading rates) in B illustrates a two-step rheological response of the soft PMN to point loads. (For more details see the text.)

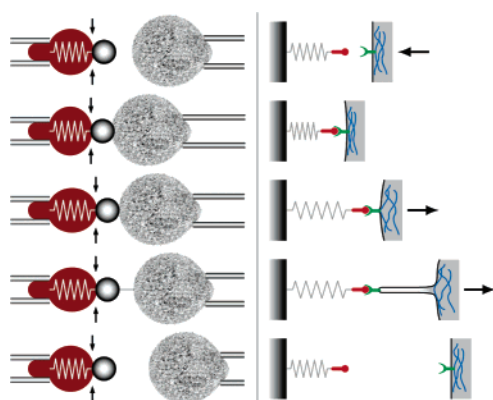


Figure 5. Sketch of a BFP:PMN test cycle²⁵ consisting of (top to bottom): (i) PMN approach, (ii) feedback-controlled touch to the BFP with formation of a P-selectin:PSGL-1 attachment, (iii) initial elastic deformation of the cell cortex upon PMN retraction, (iv) tether extrusion after release of the cytoskeletal anchor of PSGL-1, and (v) detachment and recoil of the BFP due to P-selectin:PSGL-1 dissociation. The panel on the right gives a schematic illustration of the envisioned nanomechanical processes during these steps.

nanoscale membrane tubes (“tethers”) were extruded from the neutrophil. The tethers were generally invisible, apart from an occasional funnel-shaped protrusion at the cellular tether base. As illustrated in Figure 5, we interpret the abrupt transition from elastic to plastic-like behavior at the force f_{β} as the failure of a molecular linkage that anchors the intracellular tail domain of PSGL-1 to the cortical cytostructure of the leukocyte.^{10,25} To avoid speculation, we will call this attachment in the following the “cytoskeletal anchor of PSGL-1”, without attempting to identify the exact nature of the possibly complex linkage, nor where exactly it may rupture under force.

Presuming the existence of this cytoskeletal anchor of PSGL-1 in normal neutrophils, the formation of an extracellular P-selectin:PSGL-1 adhesion bond will initially establish a membrane-spanning attachment between P-selectin and the PMN cortex, with PSGL-1 acting as a transmembrane “bridge”. Such a serial bond is an excellent candidate for a

“preprogrammed” molecular structure with functional importance in the mechanoregulation of leukocyte adhesion. Clearly, the P-selectin-mediated PMN attachment to the endothelium will terminate if the extracellular P-selectin:PSGL-1 bond fails. The force history experienced by this bond, however, is dramatically different depending on whether PSGL-1 is anchored to the cytoskeleton or not, which in turn augments the lifetime of the extracellular adhesion bond and thus the duration of the contact between the PMN and the endothelium. Our experimental approach has allowed us not only to characterize both constituents of this serial bond separately but also to quantify the directly related two-step rheological cell response to point loads. The results are summarized in the following subsections.

The P-Selectin:PSGL-1 Catch Bond – A Mechanochemical Molecular Switch that Prevents Leukocyte Arrest in Slow Flow. A peculiar shear-threshold behavior^{31–33} of rolling neutrophils or test particles has frequently been observed in flow-chamber experiments. Below a certain shear rate, the lifetimes of transient attachments of neutrophils to selectin-coated substrates did unexpectedly not increase further. Instead, the attachments appeared to become *weaker*, despite the reduced shear stresses that the cells were subjected to. Recent findings showed that this behavior can be traced directly to the molecular interaction between selectins and PSGL-1.^{24,34,35}

Figure 6 presents the dynamic force spectrum of the P-selectin:PSGL-1 bond that we measured with the setup shown in Figure 4A.²⁴ Focusing first on the filled squares, a clear logarithmic dependence between rupture force and loading rate is seen at rates larger than ~ 300 pN/s, in close agreement with the prediction of eq 6. For this range of loading rates, the interaction is characterized by a force scale $f_{\beta} \approx 18$ pN and an apparent unstressed off-rate of $k_{\text{off},0} \approx 0.37$ s^{−1}. However, when bonds were loaded by force ramps with rates below ~ 300 pN/s, the most frequent rupture force dropped to near zero (filled upside-down triangles), in agreement with the observed shear-threshold behavior of rolling neutrophils. On the other hand, when the same slow

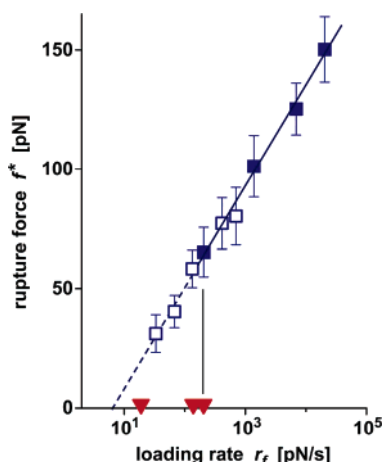


Figure 6. Most frequent rupture force (highest peak in individual histograms) as a function of the loading rate for the P-selectin:PSGL-1 bond.²⁴ Filled symbols (squares and triangles) were obtained by loading single attachments with a steady ramp of force. Empty squares were obtained using a different force protocol that consisted of an initial fast step to 20–30 pN, followed by a linear ramp at the indicated loading rate.

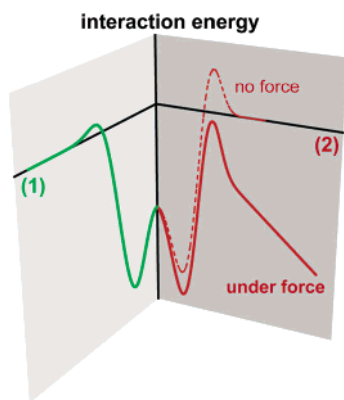


Figure 7. Conceptualized energy landscape with two separate unbinding pathways. A landscape of this form is thought to govern the P-selectin:PSGL-1 interaction.

loading rates were applied after a quick initial step in force (to 20–30 pN within 5–6 ms), the most frequent rupture force (empty squares) followed the same spectrum that had been found at high loading rates using the continuous force ramp. Clearly, the initial force jump “locked” the interaction in the bound state. Interestingly, Dembo et al. anticipated this behavior as early as 1988, calling bonds of this type “catch-slip bonds”.³⁶

These observations, and a number of additional experimental results,²⁴ led us to the conclusion that the dissociation of the P-selectin:PSGL-1 bond can occur along two distinct unbinding pathways. A conceptual view of the envisioned energy landscape underlying this behavior is shown in Figure 7. An important detail is the existence of two ground states. In the absence of force, or if the bond is loaded very slowly, the dissociation follows the “easy-out” pathway (1) across a small energy barrier. This pathway is little affected by force; hence it was sketched perpendicular to the direction of force application. On the other hand, the initially high energy barrier impeding pathway (2) as well as the second ground state are lowered by force. This gradually “empties” the ground state of path (1) and thus prevents dissociation along that pathway—as long as the force increases fast enough. Eventually, pathway (1) shuts down completely, and the

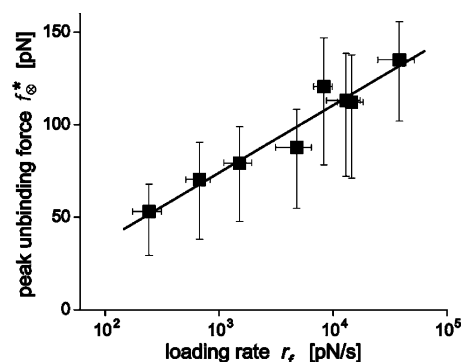


Figure 8. Most frequent transition force for release of the cytoskeletal anchor of PSGL-1 as function of the average loading rate.²⁵

situation in the (2)-direction becomes the simple, one-dimensional case discussed above in the background section on DFS.

This example demonstrates how single molecules can act as mechanochemical switches. In the present case, the strength of an important cellular adhesion bond is toggled between low and high depending on the force-loading rate. The resulting dramatic weakening of transient adhesion bonds between leukocytes and the endothelium under low shear stress is believed to prevent clogging in blood vessels where flow is slow.

The Cytoskeletal Anchor of PSGL-1 Exhibits the Signature of a Weak Chemical Bond. Using the setup shown in Figure 4B, we also collected the values of the crossover forces f_{\otimes} obtained over a 200-fold range of (average) measured loading rates into histograms.²⁵ These histograms were well described by the probability distribution eq 7, and the dynamic force spectrum of the most likely crossover forces (shown in Figure 8) revealed a linear dependence of the transition force on the logarithm of the loading rate, as predicted by eq 6. This good agreement between the measured crossover forces and the theoretically predicted behavior of a single, weak chemical bond is a strong indication that the transition at f_{\otimes} reflects the failure of a single linkage, i.e., the weakest link in the possibly complex molecular structure that anchors PSGL-1 to the cytoskeletal cortex of PMNs. The force scale that best characterizes this interaction was found to be $f_{\beta} \approx 17$ pN, with the apparent unstressed off-rate in the range of $k_{\text{off},0} \approx 0.7\text{--}1.7$ s⁻¹.

A Two-Step Rheological Cell Response Dramatically Decreases the Load on the Adhesion Bond. To quantify the observed two-step rheological response of PMNs to point loads,^{25,26} we have adopted the following phenomenological description of the measured force-time curves (such as shown in Figures 4B and 9). A straight line was matched to the linear force rise in the initial elastic regime (cf. Figure 9). Its slope is the measured loading rate r_f in this regime. The spring constant k_i for this elastic deformation of the PMN's cytoskeletal cortex is easily calculated as

$$k_i = k_t \frac{1}{r_f^0/r_f - 1} \quad (10)$$

recognizing that the PMN is in series with the force transducer. The subsequent approach to an apparent force

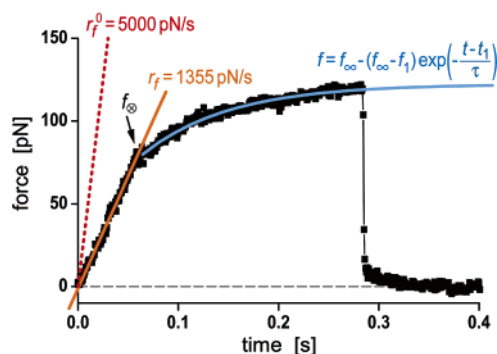


Figure 9. Phenomenological description of the typical force evolution during tensile point-loading of a neutrophil.²⁶ Pulling on a rigid structure would give a straight line with slope r_f^0 (dotted line). In contrast, the initial soft-elastic response of the PMN cortex produces a linear rise in force up to f_∞ at the measured loading rate $r_f < r_f^0$ (solid straight-line fit). Beyond f_∞ , the force approach to a rate-dependent plateau f_∞ reflects viscous tether extrusion and is well described by an exponential fit (curved solid line).

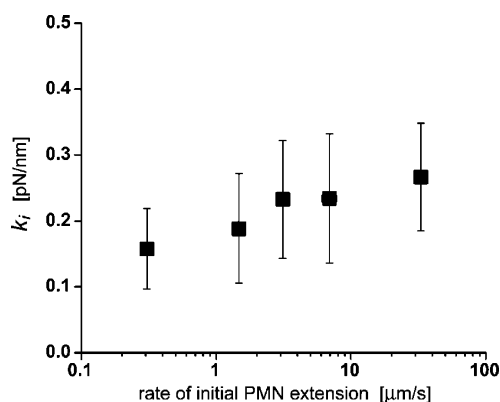


Figure 10. Spring constants for the initial soft-elastic deformation of the PMN cortex under a tensile point load.²⁵ The values were obtained from the slopes r_f of straight-line fits to the linear regime of the force-time curves (cf. Figure 9) using eq 10.

plateau was almost always well described by an exponential fit of the form (cf. Figure 9)

$$f(t) = f_\infty - (f_\infty - f_1) \exp\left(-\frac{t - t_1}{\tau}\right) \quad (11)$$

with the plateau force f_∞ and the characteristic time τ as empirical fitting parameters. (Another fitting parameter, $f_1 = f(t_1)$, is the force at the first data point of a suitably chosen fitting range.)

Figures 10 and 11 summarize the main results of this analysis. Figure 10 shows the spring constant k_i (cf. eq 10) for the initial soft-elastic response of the PMN cortex to a point load as function of the PMN extension rate. The semilog plot reveals a value of $k_i \approx 0.2$ – 0.25 pN/nm that is roughly constant over a large range of rates, as expected for ideal elastic behavior. (The apparent slight increase of the k_i -values at larger rates indicates a slow viscous component, most likely due to deformation of the whole cell.) This initial elastic regime acts to soften the impact experienced by both constituents of a serial P-selectin:PSGL-1:cytostructure attachment, i.e., the P-selectin:PSGL-1 adhesion bond as well as the cytoskeletal anchor of PSGL-1. A similar, additional effect can be expected in vivo from the softness of the vessel walls.

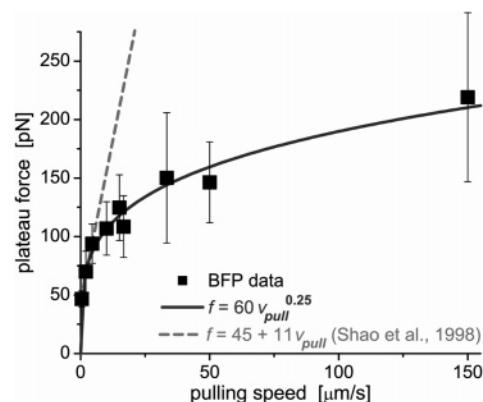


Figure 11. Tethering forces f_∞ obtained by fitting eq 11 to the exponential-like approach of the recorded force to a plateau (cf. Figure 9).²⁶ Included is the prediction by Shao et al.²⁰ for Newtonian tether flow (dashed line) obtained from tether-force measurements over a limited range of slow pulling speeds. In contrast, the power-law fit to our data (solid line) reveals a strong shear-thinning effect that reduces the tethering force at high rates considerably.

The crossover to viscoelastic behavior at f_∞ (Figures 4B and 9) causes a substantially greater reduction in the stress experienced by the P-selectin:PSGL-1 bond. In this regime, the continuing growth of the total cell extension is accompanied by an exponential-like force approach to a rate-dependent plateau f_∞ . Characteristic for tether extrusion, this apparently Maxwellian rheological response commences only after the release of the cytoskeletal anchor of PSGL-1. A plot of the tethering-plateau force as a function of the pulling speed is shown in Figure 11, where we have also included the result of pioneering studies of leukocyte-tether mechanics by Hochmuth and co-workers.²⁰ The data obtained with the biomembrane force probe reveals clearly that tether flow is not Newtonian. Instead, tether extrusion at higher rates is greatly facilitated by a shear-thinning behavior of cell material as it flows onto the tether. Obtained from a log–log plot of the BFP data, the power law

$$\frac{f_\infty}{[\text{pN}]} \approx 60 \left(\frac{v_{\text{pull}}}{[\mu\text{m/s}]} \right)^{0.25} \quad (12)$$

was the best match to the dependence of the tethering force on the full range of measured pulling speeds. We would like to emphasize that the previously published original data^{19–22} are in near-perfect agreement with our tethering forces in the respective ranges of pulling speeds. However, being able to pull tethers over an exceptional, almost 1000-fold range of speeds leads us to the reinterpretation of the leukocyte-tethering dynamics in terms of eq 12. Additional support for this shear-thinning behavior is provided by our measurements of the characteristic times τ for the exponential-like approach to a constant plateau force (cf. eq 11). The dependence of the characteristic time on pulling speed was found to follow the inverse power law

$$\frac{\tau}{[\text{s}]} \approx 0.3 \left(\frac{v_{\text{pull}}}{[\mu\text{m/s}]} \right)^{-0.75} \quad (13)$$

Mechanoregulation of Transient Leukocyte Attachments. Together, the above results allow us to predict the typical scenario for a transient PMN attachment to immobilized P-selectin. As mentioned earlier, an intact extra-

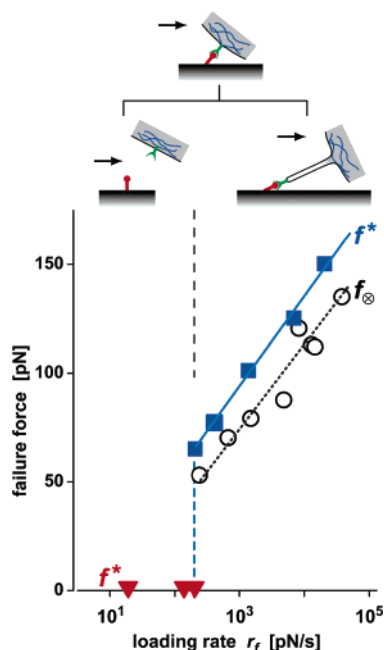


Figure 12. Combined dynamic force spectra of the two constituents of the serial transmembrane linkage.²⁶ Filled symbols (squares and triangles) mark the catch-bond response of the extracellular P-selectin:PSGL-1 adhesion bond (cf. Figure 6). Open circles are the most frequent failure forces of the cytoskeletal anchor of PSGL-1 (cf. Figure 8). The sketch at the top illustrates the dramatically different behavior depending on which part of the serial linkage fails first under a rising force load (taken here as the drag exerted by flow as denoted by the arrow). At low rates (left of the vertical dashed line), the extracellular P-selectin:PSGL-1 bond breaks first, leading to PMN detachment from immobilized P-selectin. At rates above a threshold of ~ 300 pN/s, the cytoskeletal anchor of PSGL-1 is the weaker link in the serial attachment. Its failure enables tether extrusion, which fundamentally changes the force history experienced by the still-intact P-selectin:PSGL-1 bond.

cellular P-selectin:PSGL-1 adhesion bond is a prerequisite for the existence of such an attachment. Following the formation of a P-selectin:PSGL-1 bond, the PMN is moved away from the attachment site, e.g., by the drag of the bloodstream, or in our experiments by translation of the pipet that holds the cell. During this small displacement, the elastic softness of the cellular cortex leads to a gradual, quasi-linear increase of the force experienced by the adhesion bond. The cell-translation speed (set, e.g., by the local flow rate) and the cortical softness determine the bond's force-loading rate at this stage. The loading rate, in turn, toggles a mechanochemical switch that is preprogrammed into the molecular structure of the P-selecting-PSGL-1 complex itself, determining its adhesive strength. If the loading rate is smaller than a threshold of ~ 300 pN/s, the P-selectin:PSGL-1 bond has practically no strength; consequently, the PMN detaches as depicted in Figure 12 (to the left of the vertical dashed line).

On the other hand, for loading rates above this threshold, the P-selectin:PSGL-1 bond acquires a dynamic strength that is substantially higher. The putative cytoskeletal anchor of PSGL-1 is in series with this bond; hence, both constituents of the serial linkage continue to experience the same rising force load. The dynamic force spectra for failure of these two linkages are combined in Figure 12. It is seen clearly that at all loading rates above ~ 300 pN/s, the most frequent failure force f^* of the P-selectin:PSGL-1 bond is *higher* than the most likely force f_∞ at which the cytoskeletal anchor of

PSGL-1 is released. In other words, the cytoskeletal anchor of PSGL-1 will most often fail *before* the rising force can reach the rupture level of the extracellular P-selectin:PSGL-1 adhesion bond. This earlier release of the cytoskeletal anchor of PSGL-1 has two dramatic consequences: (i) the force history experienced by the still-intact P-selectin:PSGL-1 bond changes completely and (ii) the PMN resumes movement at moderate speeds, covering distances that are considerably larger than its initial displacement from the attachment site.

Examples for the change in force history at f_∞ are given in Figures 4B and 9. After failure of the cytoskeletal anchor of PSGL-1, tether extrusion causes an exponential drop of the rate at which the remaining extracellular bond is loaded. The situation now resembles plastic-like flow, i.e., a quasi-constant-force displacement at fixed speed. This results in a significant increase of the mean survival time of the P-selectin:PSGL-1 bond, or equivalently, of the PMN attachment. In other words, the release of the cytoskeletal anchor of PSGL-1 and the subsequent tether flow represent a mechanical fuse that prevents premature cell detachment from immobilized P-selectin. Interestingly, the force-plateau levels (f_∞ in Figure 11) are not linearly proportional to the tether-extrusion speed. Instead, a shear-thinning tether flow causes an additional reduction in the force load exerted on any surviving P-selectin:PSGL-1 bonds at high extrusion speeds. In vivo, the resulting prolonged lifetime of PMN attachments, in combination with the extrusion of membrane tethers, will enable PMNs to move slowly downstream of the blood flow for some time. The shear flow will, at the same time, act to push the tethered PMN against the vessel wall. This gives the cell the opportunity to form new adhesive bonds with the endothelium before the current P-selectin:PSGL-1 bond eventually fails.

CONCLUSIONS

We used the biomembrane force probe to test the adhesive strengths of attachments between surface-bound P-selectin and either intact neutrophils or immobilized PSGL-1. Combining single-molecule with single-cell experiments has enabled us to paint a comprehensive picture of intriguing nano-to-micromechanical processes that play key roles in the regulation of the initial stages of leukocyte adhesion. In addition to the dependence on the bloodstream's shear rate and on the surface densities of adhesion sites,^{37,38} we have shown that the duration of endothelial contacts of a leukocyte (via P-selectin) is significantly affected by (i) the mechanochemical switch that is preprogrammed into the structure of the P-selectin:PSGL-1 complex, and that selects one of two unbinding pathways depending on the loading rate, (ii) the dynamic strength of the intracellular linkage that anchors PSGL-1 to the cortical cytoskeleton, (iii) the *relative* strengths of the above two constituents of the serial transmembrane linkage P-selectin:PSGL-1:cortical cytostructure over a broad range of force-loading rates, (iv) the two-step rheological response of soft linkers supporting the attachments, i.e., the crossover from an initial elastic extension of the PMN cortex to viscoelastic, constant-force tether flow, and (v) the additional reduction in bond load at high rates due to the shear-thinning behavior of cell material as it flows onto a tether.

Together, these mechanisms not only prevent permanent cell arrest at sites where blood flow is low but also enable

leukocytes to patrol vessel walls largely unaffected by variations in the bloodstream's flow rate in regions where this rate is above the shear threshold.

Finally, it is worthwhile to note that our force tests against intact neutrophils represent the prototype of a novel, *non-invasive* experimental technique to study *intracellular* mechanics of single cells. The technique relies on membrane-embedded macromolecules (such as PSGL-1) that act as transmembrane "handles". Forming specific extracellular attachments between such molecular handles and an ultra-sensitive force probe, we are able to inspect nano-to-microscale mechanical features inside cells, for example, the intracellular anchoring strength of adhesion receptors, or the cohesive strength of the actin cytoskeleton.

ACKNOWLEDGMENT

This work was supported by National Institutes of Health Grants HL65333 and HL31579. Permission to reprint previously published figure parts was granted by the Biophysical Society.

REFERENCES AND NOTES

- (1) Vestweber, D.; Blanks, J. E. Mechanisms that regulate the function of the selectins and their ligands. *Physiol. Rev.* **1999**, *79*, 181–213.
- (2) McEver, R. P. Adhesive interactions of leukocytes, platelets, and the vessel wall during hemostasis and inflammation. *Thromb. Haemost.* **2001**, *86*, 746–756.
- (3) McEver, R. P. Selectins: lectins that initiate cell adhesion under flow. *Curr. Opin. Cell. Biol.* **2002**, *14*, 581–586.
- (4) Simon, S. I.; Green, C. E. Molecular Mechanics and Dynamics of Leukocyte Recruitment During Inflammation. *Annu. Rev. Biomed. Eng.* **2004**.
- (5) Somers, W. S.; Tang, J.; Shaw, G. D.; Camphausen, R. T. Insights into the molecular basis of leukocyte tethering and rolling revealed by structures of P- and E-selectin bound to SLe(X) and PSGL-1. *Cell* **2000**, *103*, 467–479.
- (6) Evans, E.; Ritchie, K. Dynamic strength of molecular adhesion bonds. *Biophys. J.* **1997**, *72*, 1541–1555.
- (7) Evans, E.; Williams, P. M. Dynamic force spectroscopy: I. single bonds. In *Physics of Bio-Molecules and Cells, Ecoles des HOUCES d'Ete LXXV*; EDP Sciences – Springer-Verlag: 2002; pp 145–185.
- (8) Evans, E.; Ritchie, K.; Merkel, R. Sensitive force technique to probe molecular adhesion and structural linkages at biological interfaces. *Biophys. J.* **1995**, *68*, 2580–2587.
- (9) Merkel, R.; Nassoy, P.; Leung, A.; Ritchie, K.; Evans, E. Energy landscapes of receptor–ligand bonds explored with dynamic force spectroscopy. *Nature* **1999**, *397*, 50–53.
- (10) Snapp, K. R.; Heitzig, C. E.; Kansas, G. S. Attachment of the PSGL-1 cytoplasmic domain to the actin cytoskeleton is essential for leukocyte rolling on P-selectin. *Blood* **2002**, *99*, 4494–4502.
- (11) Waugh, R. E. Surface viscosity measurements from large bilayer vesicle tether formation. II. Experiments. *Biophys. J.* **1982**, *38*, 29–37.
- (12) Waugh, R. E.; Song, J.; Svetina, S.; Zeks, B. Local and nonlocal curvature elasticity in bilayer membranes by tether formation from lecithin vesicles. *Biophys. J.* **1992**, *61*, 974–982.
- (13) Heinrich, V.; Waugh, R. E. A piconewton force transducer and its application to measurement of the bending stiffness of phospholipid membranes. *Ann. Biomed. Eng.* **1996**, *24*, 595–605.
- (14) Heinrich, V.; Bozic, B.; Svetina, S.; Zeks, B. Vesicle deformation by an axial load: From elongated shapes to tethered vesicles. *Biophys. J.* **1999**, *76*, 2056–2071.
- (15) Hochmuth, R. M.; Wiles, H. C.; Evans, E. A.; McCown, J. T. Extensional flow of erythrocyte membrane from cell body to elastic tether. II. Experiment. *Biophys. J.* **1982**, *39*, 83–89.
- (16) Dai, J.; Sheetz, M. P. Mechanical properties of neuronal growth cone membranes studied by tether formation with laser optical tweezers. *Biophys. J.* **1995**, *68*, 988–996.
- (17) Hochmuth, R. M.; Shao, J. Y.; Dai, J.; Sheetz, M. P. Deformation and flow of membrane into tethers extracted from neuronal growth cones. *Biophys. J.* **1996**, *70*, 358–369.
- (18) Dai, J.; Sheetz, M. P. Membrane tether formation from blebbing cells. *Biophys. J.* **1999**, *77*, 3363–3370.
- (19) Shao, J. Y.; Hochmuth, R. M. Micropipette suction for measuring piconewton forces of adhesion and tether formation from neutrophil membranes. *Biophys. J.* **1996**, *71*, 2892–2901.
- (20) Shao, J. Y.; Ting-Beall, H. P.; Hochmuth, R. M. Static and dynamic lengths of neutrophil microvilli. *Proc. Natl. Acad. Sci. U.S.A.* **1998**, *95*, 6797–6802.
- (21) Marcus, W. D.; Hochmuth, R. M. Experimental studies of membrane tethers formed from human neutrophils. *Ann. Biomed. Eng.* **2002**, *30*, 1273–1280.
- (22) Schmidtke, D. W.; Diamond, S. L. Direct observation of membrane tethers formed during neutrophil attachment to platelets or P-selectin under physiological flow. *J. Cell Biol.* **2000**, *149*, 719–730.
- (23) Ramachandran, V.; Williams, M.; Yago, T.; Schmidtke, D. W.; McEver, R. P. Dynamic alterations of membrane tethers stabilize leukocyte rolling on P-selectin. *Proc. Natl. Acad. Sci. U.S.A.* **2004**, *101*, 13519–13524.
- (24) Evans, E.; Leung, A.; Heinrich, V.; Zhu, C. Mechanical switching and coupling between two dissociation pathways in a P-selectin adhesion bond. *Proc. Natl. Acad. Sci. U.S.A.* **2004**, *101*, 11281–11286.
- (25) Evans, E.; Heinrich, V.; Leung, A.; Kinoshita, K. Nano- to microscale dynamics of P-selectin detachment from leukocyte interfaces. I. Membrane separation from the cytoskeleton. *Biophys. J.* **2005**, *88*, 2288–2298.
- (26) Heinrich, V.; Leung, A.; Evans, E. Nano- to microscale dynamics of P-selectin detachment from leukocyte interfaces. II. Tether flow terminated by P-selectin dissociation from PSGL-1. *Biophys. J.* **2005**, *88*, 2299–2308.
- (27) Evans, E.; Leung, A.; Hammer, D.; Simon, S. Chemically distinct transition states govern rapid dissociation of single L-selectin bonds under force. *Proc. Natl. Acad. Sci. U.S.A.* **2001**, *98*, 3784–3789.
- (28) Kramers, H. Brownian motion in a field of force and the diffusion model of chemical reactions. *Physica (Utrecht)* **1940**, *7*, 284.
- (29) Bell, G. I. Models for the specific adhesion of cells to cells. *Science* **1978**, *200*, 618–627.
- (30) Simson, D. A.; Ziemann, F.; Strigl, M.; Merkel, R. Micropipet-based pico force transducer: in depth analysis and experimental verification. *Biophys. J.* **1998**, *74*, 2080–2088.
- (31) Finger, E. B.; Puri, K. D.; Alon, R.; Lawrence, M. B.; von Andrian, U. H.; Springer, T. A. Adhesion through L-selectin requires a threshold hydrodynamic shear. *Nature* **1996**, *379*, 266–269.
- (32) Alon, R.; Chen, S.; Fuhlbrigge, R.; Puri, K. D.; Springer, T. A. The kinetics and shear threshold of transient and rolling interactions of L-selectin with its ligand on leukocytes. *Proc. Natl. Acad. Sci. U.S.A.* **1998**, *95*, 11631–11636.
- (33) Greenberg, A. W.; Brunk, D. K.; Hammer, D. A. Cell-free rolling mediated by L-selectin and sialyl Lewis(x) reveals the shear threshold effect. *Biophys. J.* **2000**, *79*, 2391–2402.
- (34) Marshall, B. T.; Long, M.; Piper, J. W.; Yago, T.; McEver, R. P.; Zhu, C. Direct observation of catch bonds involving cell-adhesion molecules. *Nature* **2003**, *423*, 190–193.
- (35) Yago, T.; Wu, J.; Wey, C. D.; Klopocki, A. G.; Zhu, C.; McEver, R. P. Catch bonds govern adhesion through L-selectin at threshold shear. *J. Cell Biol.* **2004**, *166*, 913–923.
- (36) Dembo, M.; Torney, D. C.; Saxman, K.; Hammer, D. The reaction-limited kinetics of membrane-to-surface adhesion and detachment. *Proc. R. Soc. London, Ser. B* **1988**, *234*, 55–83.
- (37) Lawrence, M. B.; Springer, T. A. Leukocytes roll on a selectin at physiologic flow rates: distinction from and prerequisite for adhesion through integrins. *Cell* **1991**, *65*, 859–873.
- (38) Brunk, D. K.; Hammer, D. A. Quantifying rolling adhesion with a cell-free assay: E-selectin and its carbohydrate ligands. *Biophys. J.* **1997**, *72*, 2820–2833.

CI0501903